International Journal of Biological Macromolecules 334 (2025) 149060

Contents lists available at ScienceDirect

International Journal of Biological Macromolecules

journal homepage: www.elsevier.com/locate/ijbiomac

# Enhancement of mechanical and optical properties of modified chitosan films via grafting of multiple hydrogen bonding motifs

Mouad El Mouzahim [a], Alessandro Pedrini [a], Enrico Dalcanale [a], A. Jorge Parola [b], Roberta Pinalli [a,*,1]

[a] Department of Chemistry, Life Sciences and Environmental Sustainability, University of Parma, INSTM, UdR Parma, Parco Area delle Scienze 17/A, Parma, 43124, Italy

[b] LAQV-REQUIMTE, Department of Chemistry, Faculty of Sciences and Technology, New University of Lisbon, 2829-516, Caparica, Portugal

ARTICLE INFO

*Keywords:*
Chitosan
Self-dimerizing ODIN
Multiple hydrogen bonding
UV barrier

ABSTRACT

This study explores enhancing chitosan film (Cs) properties via supramolecular H-bonding cross-linking. The first unit, (1-(7-oxo-7,8-dihydro-1,8-naphtiridin-2-yl)urea (ODIN), was selected for its ability to self-dimerize via a sextuple H-bonding motif, while the second unit, phenyl urea (PU), was chosen as non-dimerizing unit that is still capable of forming extensive H-bonds. FTIR analysis confirmed the successful incorporation of ODIN and PU into the chitosan skeleton. The mechanical and barrier properties, and UV protection performances of the two modified polymers were determined and compared with those of pristine chitosan. These modifications resulted in enhanced surface hydrophobicity, and a substantial decrease in water vapor permeability. Mechanical testing revealed substantial reinforcement, with tensile strength increasing by up to 200 % for ODIN-modified films and up to 100 % for PU-modified ones. The UV-blocking performance of Cs-ODIN films was notably enhanced, providing complete protection across UVA, UVB, and UVC wavelengths, achieving a UPF of 161.95. The UV protective effect was further validated using the red cabbage test, which proved that Cs-ODIN films markedly reduced color degradation under UV exposure. Overall, this study shows that while PU mainly enhances barrier properties and mechanical performance through additional hydrogen-bonding interactions, ODIN not only provides similar improvements but also offers further benefits, including (i) enhanced UV-shielding and (ii) superior toughness and thermal stability driven by supramolecular dimerization.

## 1. Introduction

Chitosan, a linear polysaccharide derived from the partial deacetylation of chitin found in the exoskeletons of marine crustaceans, is characterized by the repeated units of β-(1 → 4)-linked D-glucosamine and *N*-acetyl-D-glucosamine. It is the only abundant natural polysaccharide that carries a positive charge [1], and is recognized for its biocompatibility, biodegradability, non-toxicity, and antimicrobial activity [2]. Owing to these properties, chitosan has found applications in diverse fields, including drug delivery, gene therapy, cosmetics, bioimaging, and increasingly in food packaging [3–6]. Nevertheless, the pristine polymer exhibits limitations in physicochemical and mechanical properties, which can be enhanced with both physical and chemical modification strategies [7]. Chemical modification is an appealing and effective approach to improve chitosan characteristics, thanks to the presence of reactive amino (–$NH_2$) and hydroxyl (–OH) groups [8]. Common chemical modification methods include sulfonation, alkylation, esterification, carboxylation, and Schiff base formation [7,9–12].

Chitosan has recently gained significant attention as a sustainable alternative for food packaging [13–15]. In such applications, adequate tensile strength is required to prevent tearing and ensure package integrity during handling. Additionally, evaluating barrier properties against water vapor and UV radiation is crucial to limit moisture transfer and avoid light-induced oxidation, both of which directly affect product shelf life [16].

However, for food packaging, physical modification techniques, such as the incorporation of plant extracts [14,15], essential oils (EOs) [17,18], nanoparticles [19,20], or blending with other polymers [14] are often preferred due to their simplicity and compliance with food safety standards, yet these physical modifications suffer from limited

* Corresponding author.
*E-mail address:* roberta.pinalli@unipr.it (R. Pinalli).
[1] Scopus Author ID: 6506474623.

https://doi.org/10.1016/j.ijbiomac.2025.149060
Received 18 September 2025; Received in revised form 6 November 2025; Accepted 14 November 2025
Available online 19 November 2025

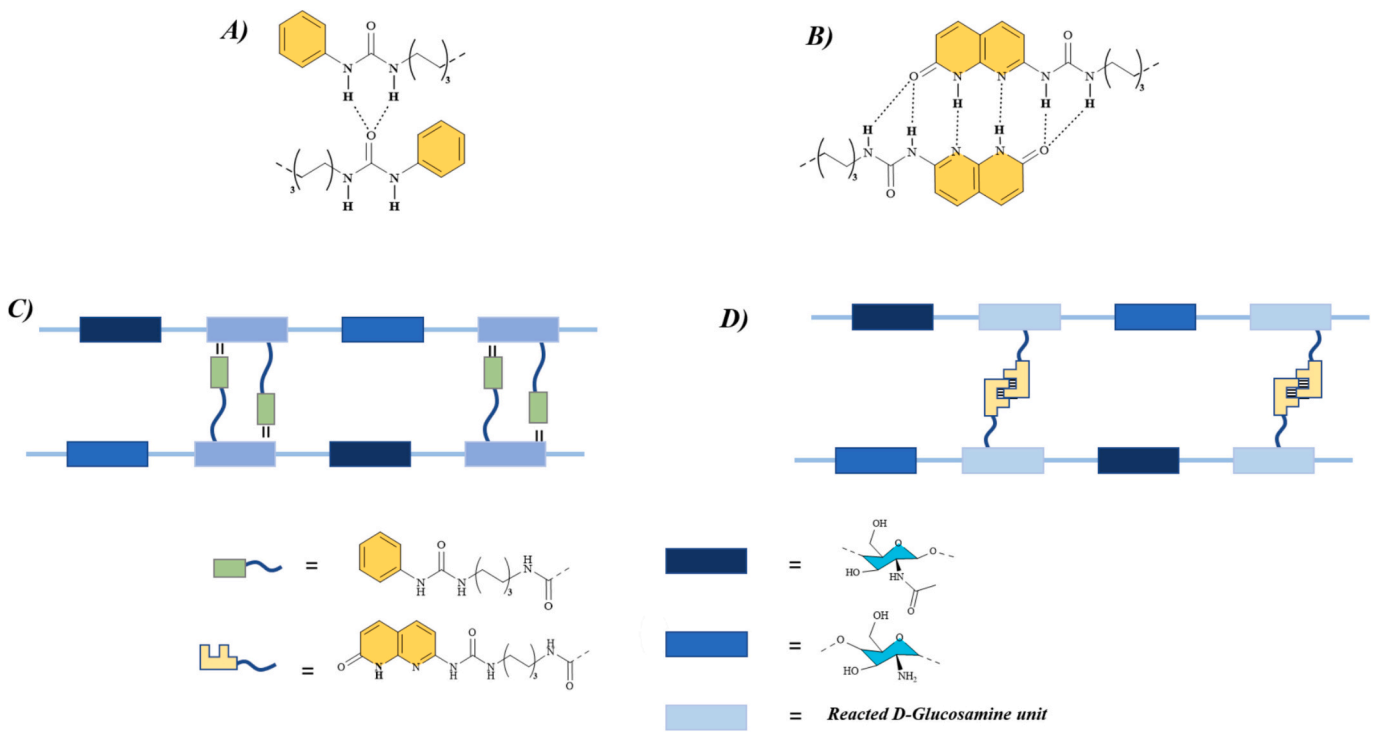


**Chart 1.** (A) PU H-bonding network; (B) ODIN self-dimerizing unit. Representation of the modified-Cs matrix reinforced with PU (C) and ODIN dimer (D). The different H-bonding motifs are sketched in the chart.

long-term stability, as the incorporated components may gradually leach out or lose functionality over time [21].

In this study, we investigated the chemical grafting of specific molecules developed and previously reported by us, which are 1-(7-oxo-7,8-dihydro-1,8-naphthyridin-2-yl)urea) (ODIN) [22] and a phenyl urea (PU) derivative [23], for enhancing the mechanical performance and barrier properties of chitosan. These moieties (Chart 1) act as efficient and reversible crosslinking agents [22].

ODIN exhibits a pronounced capacity for self-dimerization through a sextuple DDADAA (donor–donor–acceptor–donor–acceptor-acceptor) hydrogen-bonding array (Chart 1B), enabling the formation of extensive and highly stable intermolecular hydrogen-bonding networks [22,23]. In contrast, PU lacks such dimerization potential and instead forms localized hydrogen bonds with chitosan, primarily via two intramolecular N—H···O═C interactions (Chart 1A) [24,25]. In this work, PU and ODIN derivatives (Chart 1C, and D respectively) were chemically grafted onto chitosan, and the resulting modified polymers were cast into films. The effects of the modification were evaluated with respect to key material properties including mechanical strength, barrier performance, and optical characteristics.

### 1.1. Hypothesis

We hypothesize that reversibly crosslinking chitosan with the novel hydrogen-bonding motifs ODIN and PU will enhance its mechanical strength, UV shielding, and water vapor barrier properties, thanks to their ability to form supramolecular cross-links (ODIN) or extensive hydrogen bonding (PU) without the need of additional fillers. Fillers such as metal oxides or fibers can enhance their mechanical strength and moisture barrier properties. However, those fillers can pose risks such as chemical migration into food, potential toxicity from metal-based additives, and reduced biodegradability, undermining sustainability and safety goals [26], disadvantages that can be surpassed by this chemical modification.

## 2. Material and methods

### 2.1. Materials

Chitosan (Cs, purity 85–90 %, degree of deacetylation ≥80 %, molecular weight 10–15 kDa, viscosity 20–100 mPa·s in 0.5 % acetic acid at 20 °C) and hexamethylene diisocyanate (HMDI, ≥98 % purity) were purchased from TCI (USA). Glacial acetic acid (purity ≥99.7 %), 1,1-diphenyl-2-picrylhydrazyl (DPPH, purity ≥95 %), dibutyltin dilaurate (DBTL, purity ≥95 %), aniline (purity ≥99 %), 2,6-diaminopyridine (purity ≥98 %), and malic acid (purity ≥99 %) were obtained from Sigma-Aldrich (USA). It is noteworthy that all additional reagents and solvents utilized in this study were of analytical grade and did not undergo further purification.

All the reactions were performed under room light conditions.

### 2.2. Preparation of 1-(5-isocyanatopentyl)-3-phenylurea (PU)

Aniline was subjected to a reaction with an excess of hexamethylene diisocyanate (9 equivalents) within an inert atmosphere with ambient temperature maintained for a period of 4 h. The product was precipitated using cyclohexane, filtered, and washed with cyclohexane to remove unreacted HDI. The resulting white solid was dried under vacuum and characterized by $^{1}$H NMR (see Fig. S2).

### 2.3. Preparation of 1-(6-isocyanatohexyl)-3-(7-oxo-7,8-dihydro-1,8-naphthyridin-2-yl)urea (ODIN)

ODIN was synthesized following a reported procedure [22]. Naphthyridine was first prepared by reacting diaminopyridine with malic acid in concentrated $H_2SO_4$ at 110 °C for 2.5 h, then neutralized with concentrated $NH_3$ and washed with water to yield a brown solid. This intermediate was then reacted with excess hexamethylene diisocyanate (10 eq) under reflux at 118 °C for 15 h. The resulting solid was filtered, washed with hexane and acetone, and dried under vacuum to afford ODIN as a powder, characterized by $^{1}$H NMR (see Fig. S3).

### 2.4. Preparation of Cs-PU and Cs-ODIN modified polymers

5 g of chitosan powder were suspended in 50 mL dry DMSO, followed by the addition of 3 drops of dibutyltin dilaurate (DBTL) as a catalyst. ODIN or PU was then introduced in varying ratios, as reported in Table S1. The percentage of added PU and ODIN were rationalized to preserve the polymer solubility. The reaction mixture was stirred at 250 rpm for 6 h at 80 °C. Upon completion, the modified polymer was recovered by filtration, thoroughly washed with DMSO to remove unreacted compounds, and subsequently dried under vacuum at 80 °C. The resulting products were denoted as Cs-ODIN-I, Cs-ODIN-II, and Cs-ODIN-III, or Cs-PU-I, Cs-PU-II, and Cs-PU-III, corresponding to increasing amounts of ODIN or PU used during the modification process. To assess grafting efficiency, UV calibration curves of ODIN and PU in DMSO were established and employed to quantify the unreacted fractions recovered during the washing steps (Figs. S4 and S5). To confirm the successful grafting process, the Fourier-transform infrared spectrum (FTIR) of the chemically modified chitosan powders was recorded using a PerkinElmer FT-IR Spectrum Two spectrometer in Attenuated Total Reflectance (ATR) detection mode. This was performed over spectral ranges of 4000–400 cm-1, employing a resolution of 4 cm-1 and an average of 32 scans per sample. Then, the background spectra were subtracted from all measurements.

### 2.5. Films preparation

Chitosan films were prepared using the solvent casting technique. Polymer solutions were obtained by dissolving 1 % (w/v) of chitosan powder in a 1 % (v/v) aqueous acetic acid solution, followed by continuous stirring at room temperature until complete dissolution. The resulting solutions were cast into polystyrene dishes and dried at 40 °C for 48 h.

### 2.6. Films characterization

#### 2.6.1. Thickness, color, and UV barrier properties

To calculate the thickness of the films a digital micrometer (Wenzhou Sanhe Measuring Instrument Co., Ltd., Zhejiang, China) was used with a precision of 1 μm. At the same time, color parameters — $L$ (lightness), $a$ (red-green axis), and $b$ (yellow-blue axis) — were extracted using ImageJ software along with the Color Converter plugin. The total color difference (ΔE), whiteness index (*WI*), and yellowness index (*YI*) were then calculated using the corresponding standard equations [27].

$$\Delta E = \sqrt{\left[(L^* - L)^2 + (a^* - a)^2 + (b^* - b)^2\right]} \tag{1}$$

$$WI = 100 - \sqrt{\left[(100 - L)^2 + a^2 + b^2\right]} \tag{2}$$

$$YI = 142.86\, x \left(\frac{b}{L}\right) \tag{3}$$

where $\boldsymbol{L}^* = 90.32$, $\boldsymbol{a}^* = -0.01$, $\boldsymbol{b}^* = 3.64$, represent the color parameters of a standard plate with a white color that served as reference values, while $L$, $a$, and $b$ represented the color parameter values of the film sample.

The UV–visible shielding capacity of the films were assessed by recording transmittance spectra in transmission mode using a Varian Cary 300 UV–vis spectrophotometer equipped with a solid sample holder. Film opacity was determined based on the absorbance at 600 nm, calculated using Eq. (4) [27,28].

$$\text{Opacity}\ (\text{mm}^{-1}) = \frac{\text{Abs (at 600 nm)}}{\text{thickness (mm)}} \tag{4}$$

UV barrier performance was evaluated in accordance with the AS/NZS 4399 standard, which includes the calculation of UVA and UVB transmittance, as well as the ultraviolet protection factor (UPF), using Eqs. (5), (6), and (7) [29,30].

$$\text{UVA}\ (\%) = \frac{T_{315} + T_{320} + \ldots T_{400}}{18} \tag{5}$$

$$\text{UVB}\ (\%) = \frac{T_{290} + T_{295} + \ldots T_{315}}{6} \tag{6}$$

$$\text{UPF} = \frac{\sum_{290}^{400} E_\lambda \times S_\lambda \times \Delta_\lambda}{\sum_{290}^{400} E_\lambda \times S_\lambda \times T_\lambda \times \Delta_\lambda} \times 100 \tag{7}$$

where $T_\lambda$ represents the sample's spectral transmittance at a given wavelength (λ in nm); $E_\lambda$ is the relative erythemal spectral effectiveness (refer to Table B1 in AS/NZS 4399 [29]); $S_\lambda$ represents the solar spectral irradiance (refer to Table B2 in AS/NZS 4399 [29]), and Δλ indicates the wavelength increment (in nm). These symbols play a defined role in calculations according to the AS/NZS 4399 standards.

Additionally, a qualitative protection test was performed using a paper strip impregnated with UV-sensitive nitrospiropyran dye that changes to blue upon exposure to UV light. The films were placed as barriers over the dye-treated paper to assess their effectiveness in preventing dye activation.

#### 2.6.2. Moisture content and water vapor permeability

The moisture content of the films was determined gravimetrically by drying the samples at 100 °C until a stable weight was reached. The final moisture content was then calculated using Eq. (8) [28]:

$$\textit{Moisture content}(\%) = \frac{(W_f - W_0)}{W_0} \times 100 \tag{8}$$

where $W_f$ (g) represents the sample weight after the drying procedure, while $W_0$ (g) corresponds to the initial dry weight of the sample.

Water vapor permeability (WVP) of the films was evaluated based on the procedure described by J. Liu et al. [27] and X. Zhang et al. [28], with slight modifications. Film samples were securely sealed over the openings of 15 mL centrifuge tubes, effectively serving as a barrier or "lid." The tubes, containing calcium chloride as a desiccant, were then placed in a desiccator at ambient temperature alongside a beaker of distilled water to create a controlled humidity environment. After 24 h, the tubes were reweighed, and WVP was calculated using Eq. (9).

$$WVP\ \left(g.m^{-1}.s^{-1}.Pa^{-1}\right) = \frac{m \times x}{t \times S \times \Delta P} \tag{9}$$

where, $W$ (g) is the augmented mass of the tube, $x$ (m) denotes the thickness of the film, $t$ (s) represents the duration of the test, $S$ ($m^2$) signifies the surface area of the film sample, and $\Delta P$ (Pa) denotes the partial water vapor pressure (in Pascals) at a temperature of 20 °C.

#### 2.6.3. Mechanical properties

Mechanical properties of the films, including tensile strength, elongation at break, and Young's modulus, were evaluated using a TMS-Pro Advanced texture analyzer, following the protocol outlined by J. Liu et al. [27] with slight modifications. Film strips measuring 60 × 5 mm were clamped between the grips set 35 mm apart, and the test was conducted at a crosshead speed of 6 mm/min using a 50 N load cell.

#### 2.6.4. Scanning electron microscopy (SEM)

Surface morphology of the films was examined using a TM4000 Tabletop Scanning Electron Microscope (Hitachi, Japan), with 15 kV as accelerating voltage. The samples were fixed on metal support using double-sided carbon adhesive tape and subsequently coated with a thin layer of gold to ensure conductivity. SEM images were captured at a

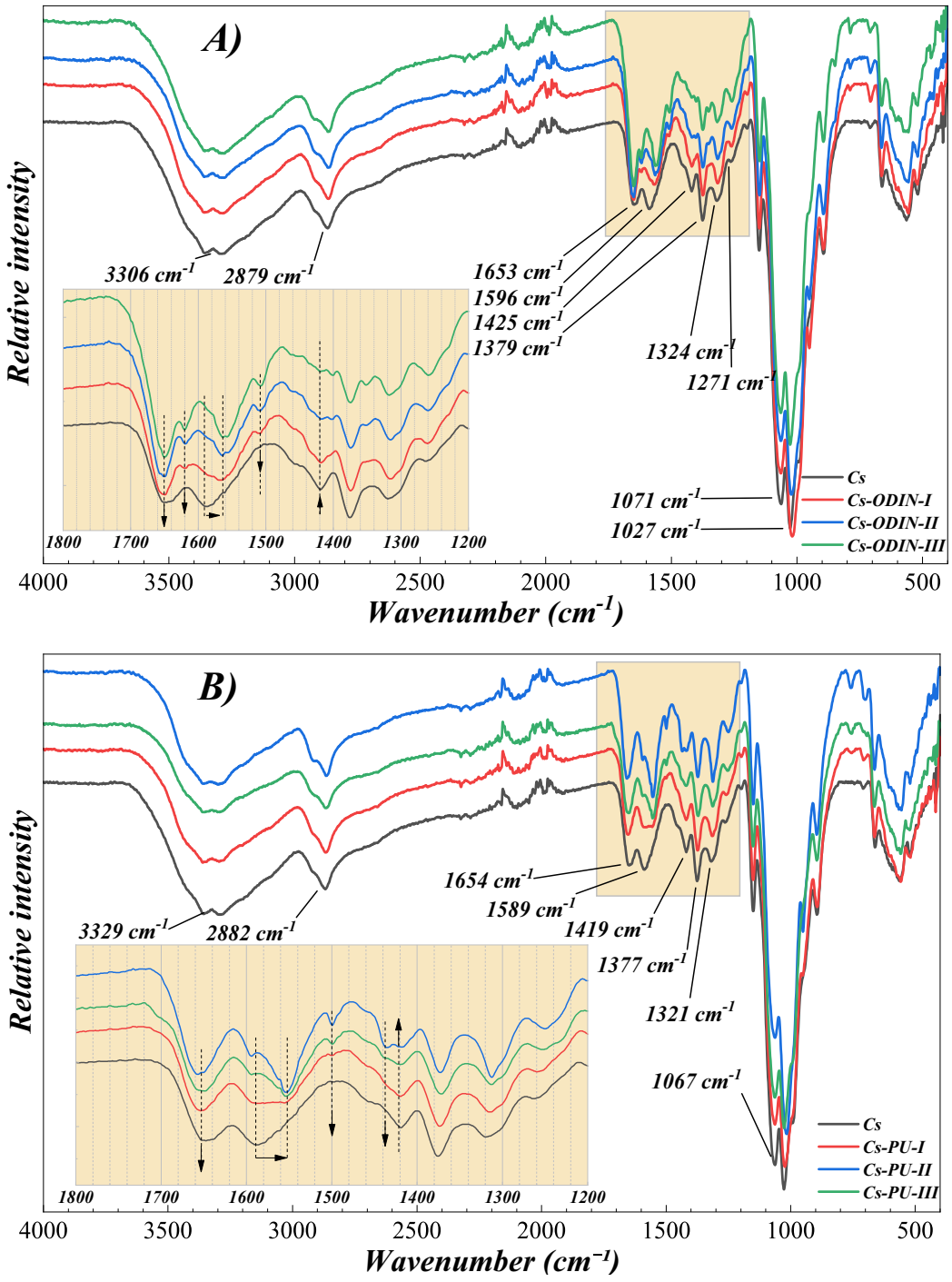


**Fig. 1.** FT-R spectrum of Cs-ODIN (A) and Cs-PU (B) films. (Yellow inset: magnification of the region between 1200 $cm^{-1}$ and 1800 $cm^{-1}$.)

magnification of 1000×.

### 2.6.5. Thermal stability

Thermogravimetric analysis (TGA) was carried out using a Perkin Elmer TGA 8000 equipped with a GC10 gas controller (pure air/nitrogen), Mettler Toledo. The samples were heated from 30 °C to 800 °C at a constant heating rate of 10 °C/min. In addition to the TGA curves, derivative thermogravimetric (DTG) curves were also calculated to obtain the degradation rate and identify the temperatures at which the maximum weight loss occurred.

### 2.6.6. Antioxidant activity

The antioxidant activity of the films was assessed using the DPPH radical scavenging assay following the method of Wang et al. [31]. Film samples, each 0.5 cm in diameter and of equal weight, were immersed in 4 mL of a $1 \times 10^{-4}$ M DPPH solution in methanol and incubated at room temperature for 4 h in the dark. The absorbance of the resulting solution was measured at 517 nm, and the radical scavenging activity was calculated using Eq. (10):

$$\text{DPPH radical scavenging activity } (\%) = \frac{(A_0 - A_1)}{A_0} \times 100 \quad (10)$$

where $A_0$ is the absorbance of the blank solution, while and $A_1$ is the

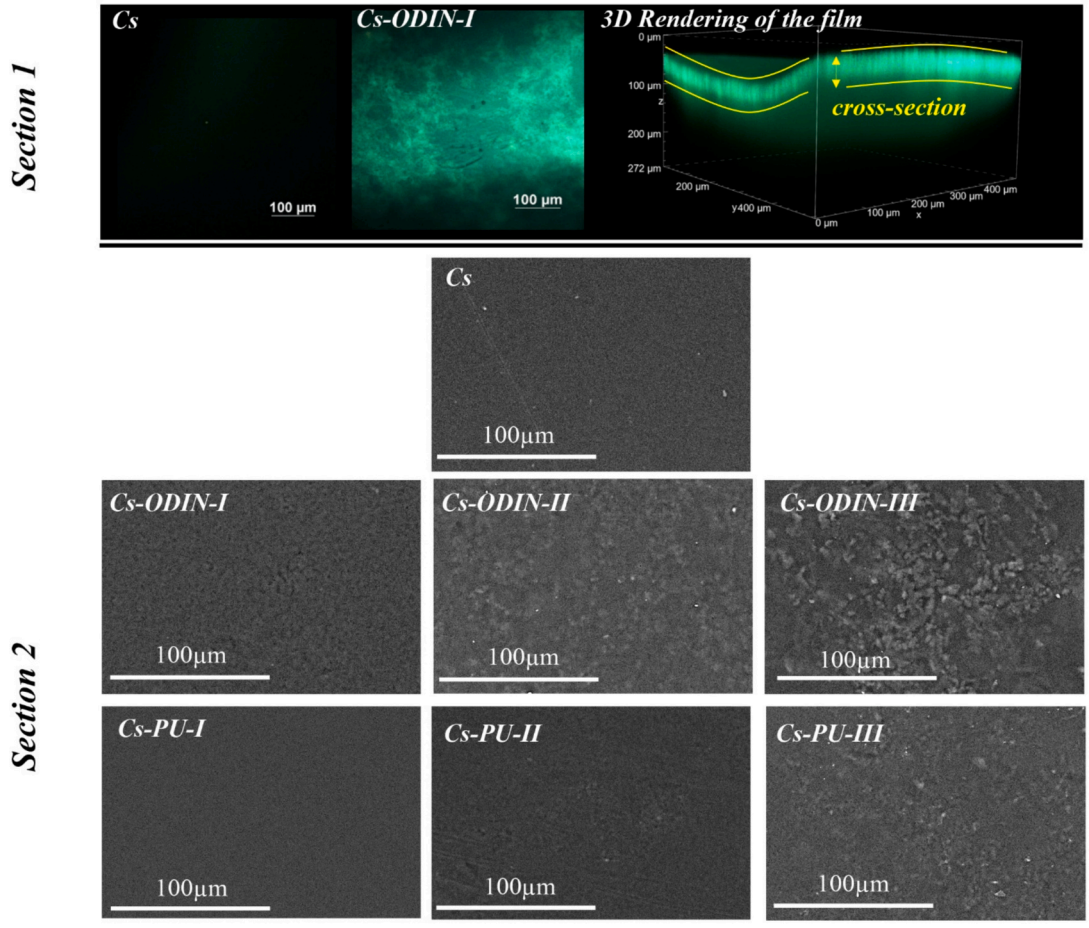


**Fig. 2.** 2-Photon microscopy images for Cs and Cs-ODIN-I films (section 1) and SEM micrographs of Cs films (section 2)

absorbance of the sample.

*2.6.7. Two-photon microscopy (2PM)*

Two-photon fluorescence imaging was carried out using a Nikon A1R MP+ Upright Microscope equipped with a Coherent Chameleon Discovery femtosecond laser (~100 fs pulse, 80 MHz, 660–1320 nm tunable range). A 25× water-dipping objective (N.A. 1.1, working distance 2.0 mm) was used for excitation and signal collection. Due to the thin-film nature of the samples, imaging was performed in air, which reduced the effective N.A. and thus the resolution, but prevented water-induced artifacts.

*2.6.8. Contact angle measurements*

Water contact angle (WCA) values of each film were measured using a Biolin Scientific Attension Theta Flex goniometer. A 4 µL droplet of distilled water was placed on three separate spots on each film, and the contact angles were recorded with a high-speed digital camera.

*2.6.9. Food preservation test (FPT)*

To assess the practical potential of the developed Cs films, a preliminary food preservation test was performed using red cabbage as a model system. Part of the cabbage surface was covered with the modified film, while the remaining portion remained uncovered. The sample was then exposed to continuous UV irradiation for 6 h to mimic oxidative stress conditions commonly encountered during food storage.

*2.7. Statistical analysis*

The experimental data were then subjected to statistical analysis using ORIGIN LAB 8.5 software. Subsequently, one-way analysis of variance (ANOVA) was employed to detect any statistically significant differences among the factors and levels, with Tukey's post hoc test for multiple comparisons then being used to ascertain the statistical significance at a level of $p < 0.05$. Each treatment underwent at least three replicates, and the results are expressed as the mean ± standard deviation (SD).

## 3. Result and discussion

*3.1. FTIR analysis*

Chitosan was chemically modified with ODIN or PU moieties through an addition reaction between the isocyanate groups present on ODIN or PU, and the hydroxyl and amino groups of chitosan. The reactivity of hydroxyl groups was enabled by using an appropriate catalyst, thereby facilitating a broader grafting pattern. The resulting solid products were recovered by filtration and extensively washed with DMSO to remove unreacted ODIN or PU. The modified chitosan was subsequently characterized by FTIR spectroscopy to confirm successful functionalization.

FTIR spectroscopy was conducted to verify the successful incorporation of ODIN into the chitosan matrix and to elucidate the nature of their interactions. Fig. 1 compares the FTIR spectra of pristine chitosan and Cs-ODIN polymers, revealing notable changes in vibrational bands across different ODIN loadings. Distinct alterations were observed particularly in the 1800–1200 $cm^{-1}$ range, providing insight into the Cs/ODIN interactions. The characteristic C═O stretching of chitosan appears at 1653 $cm^{-1}$ [32], while a new peak at 1620 $cm^{-1}$, which

**Table 1**
Thickness, Moisture, WVP of Modified-Cs Films.

| Samples | Thickness (μm) | Moisture (%) | WVP ($\times 10^{-11}$ g·m$^{-1}$·Pa$^{-1}$·s$^{-1}$) |
|---|---|---|---|
| ***Cs*** | 38.4 ± 1.8 | 13.6 ± 0.5 | 4.55 ± 0.08 |
| ***Cs-ODIN-I*** | 39.1 ± 1.2 | 13.9 ± 0.5 | 2.58 ± 0.15 |
| ***Cs-ODIN-II*** | 40.7 ± 1.9 | 14.4 ± 0.6 | 2.48 ± 0.09 |
| ***Cs-ODIN-III*** | 42.1 ± 1.8 | 13.3 ± 0.6 | 2.44 ± 0.11 |
| ***Cs-PU-I*** | 39.1 ± 0.9 | 14.1 ± 0.6 | 2.65 ± 0.23 |
| ***Cs-PU-II*** | 40.4 ± 1.8 | 14.7 ± 0.6 | 2.60 ± 0.10 |
| ***Cs-PU-III*** | 41.5 ± 1.1 | 14.2 ± 0.6 | 2.50 ± 0.09 |

Data are expressed as mean ± SD. Measurements were performed in quintuplicate for film thickness and in triplicate for both moisture content and water vapor permeability (WVP).

intensifies with increasing ODIN content, corresponds to the C═O group of ODIN. Additionally, the N—H bending peak of chitosan at 1596 cm$^{-1}$ [32] exhibited a shift toward lower wavenumbers (~1560 cm$^{-1}$) at higher ODIN concentrations. Moreover, the increasing intensity of the C═C of ODIN aromatic stretching at 1507 cm$^{-1}$ further supports the successful incorporation of ODIN into the polymer network. Similarly, Cs-PU films showed notable changes in their IR spectra depending on the PU content. An increase in the intensity of the C═O peak at 1655 cm$^{-1}$, corresponding to the carbonyl (C=O) groups of the urea linkage, along with the appearance of a C═C peak at 1502 cm$^{-1}$, attributed to the aromatic C═C bonds from PU, confirmed the presence of PU. Additionally, the Cs N—H absorption band shifted from 1590 cm$^{-1}$ to 1550 cm$^{-1}$ upon PU addition, with this shift becoming more pronounced at higher PU concentrations, as already evidenced in the case of ODIN.

### 3.2. Spectroscopic evidence of ODIN dimerization in the films

Two-photon microscopy was employed to investigate the presence of ODIN dimers within the bulk Cs polymer. The different fluorescence signature of ODIN dimer with respect to its monomer enables the visualization of the dimer distribution in the film [23]. As demonstrated in the XY view images recorded at 3 % laser power (Fig. 2 section 1), the pristine Cs film exhibited minimal fluorescence. This is due to the fact that native chitosan lacks significant intrinsic fluorescence at the excitation wavelength employed in two-photon microscopy. In contrast, the Cs-ODIN-I film exhibited a substantial increase in fluorescence intensity, accompanied by a homogeneous distribution. The observed green fluorescence of the film supports the presence of ODIN dimers, given that ODIN emits blue fluorescence in its monomeric form, while its dimeric form displays green-yellow emission [23]. The variation in fluorescence intensity across the film suggests that ODIN molecules form dimers and tend to cluster. Nevertheless, 3D rendering confirms that ODIN is distributed throughout the entire film. SEM micrographs show clearly the effect of the incorporation of both ODIN and PU on the surface and the structure of Cs films (Fig. 2 section 2). The pristine film exhibited a smooth surface [33,34]. In contrast, the films incorporating ODIN and PU exhibited a slightly rougher surface at low concentrations. At higher concentrations, large aggregates measuring approximately 3–4 μm, likely due to clustering, became evident on the film surface.

### 3.3. Physical appearance, thickness and color parameters

As discussed in paragraph 2.4 and reported in Table S1, pristine Cs was functionalized with different amounts of ODIN or PU. The corresponding films were then prepared via solvent casting (see paragraph 2.6 for details), and their thickness was measured to evaluate any potential impact on the resulting properties as shown in Table 1. No statistically significant differences in thickness ($p > 0.05$) were observed among the films obtained from pristine and modified chitosan after the casting process. Nevertheless, a slight trend can be noted: pristine chitosan (Cs) films displayed the lowest average thickness, followed by those modified with PU (Cs-PU), and finally those modified with ODIN


**Fig. 3.** Physical appearance of modified Cs films.

(Cs-ODIN), which had the highest values. Although film thickness can influence properties such as water vapor permeability (WVP) (Eq. (9)) and tensile strength (TS) [35], the variation in thickness remains within ~10 % between the modified and pristine films. This modest variation suggests that the observed changes in WVP and TS are primarily due to the intrinsic properties of the additives [36].

Pivotal characteristics for food packaging films are color and transparency. The incorporation of these two distinct molecules resulted in films with different physical appearances (Fig. 3). The films containing PU are indistinguishable from those of pristine chitosan. In contrast, the incorporation of ODIN imparted a light-yellow color to the chitosan films, with the intensity of the yellow hue increasing as the ODIN content rose. However, higher concentrations of ODIN or PU led to a decrease in transparency due to the aggregation of these molecules that can also be observed after casting, giving a slightly harsh and light diffractive surface (Fig. 3).

Measurements of the color parameters (Table S2) indicated that all the functionalized films had an ***L*** value (lightness) close to that of the pristine Cs film, ranging between 88.94 and 83.92, confirming the light color and transparency of the films. However, the ***b*** (yellow-blue) values exhibited a significant increase in the case of ODIN, while PU incorporation had a lower effect. Moreover, the calculation of ***YI*** showed a significant increase of this value, especially in the case of Cs-ODIN, indicating a subtle yellowish hue that is increasing with high ODIN content due to the color of the compound.

### 3.4. Moisture content and water vapor permeability

Moisture content and water vapor permeability (WVP) are key parameters used to assess the interaction of chitosan films with water. Moisture content reflects the film's ability to retain water, while WVP indicates its resistance to water vapor transmission. Together, they are crucial for determining the film's suitability for applications requiring moisture control, such as food packaging.

In this study, the incorporation of ODIN and PU did not lead to a statistically significant change in the moisture content of the chitosan films (Table 1). This indicates that the overall affinity of the films toward water remained largely unaltered. Although a slight increase in moisture content was observed, it was not substantial enough ($p > 0.05$) to suggest a meaningful effect on the hydrophilic character [14].

On the other hand, the water vapor permeability (WVP), a critical parameter for evaluating the barrier performance of polymeric films,

**Table 2**
WCA values of the modified Cs films.

| Sample | WCA (°) | |
|---|---|---|
| ***Cs*** | 89.9 ± 1.9 |  |
| ***Cs-ODIN-I*** | 91.9 ± 2.0 |  |
| ***Cs-ODIN-II*** | 98.3 ± 2.1 |  |
| ***Cs-ODIN-III*** | 110.1 ± 2.3 |  |
| ***Cs-PU-I*** | 93.1 ± 2.0 |  |
| ***Cs-PU-II*** | 101.4 ± 2.2 |  |
| ***Cs-PU-III*** | 114.5 ± 2.4 | 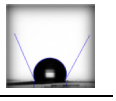 |

Data are presented as mean ± SD based on three replicates (n = 3).

especially in moisture-sensitive applications such as food packaging, cosmetics, and pharmaceutical formulations, was observed to decrease significantly following the modification ($p < 0.05$). As shown in Table 1, the incorporation of both ODIN and PU resulted in an approx. 50 % reduction in WVP compared to the pristine chitosan film. Furthermore, an increase in the concentration of ODIN and PU resulted in a slight decrease in WVP when ODIN-I and PU-I were compared with ODIN-III and PU-III, respectively. This suggests a limit in barrier enhancement, with the maximum reduction in WVP not exceeding 50 % relative to the unmodified film. This improvement is comparable to that of chitosan-based film incorporating curcumin, rice bran wax, and hydrophobic $SiO_2$ particles [13], or chitosan-based nanocomposite films incorporating covalent organic frameworks (COFs) [37]. These improvements are typically ascribed to factors such as the formation of a more tortuous diffusion path and a limited availability of free hydrophilic functional groups (e.g., –OH, $–NH_2$), all of which reduce water vapor transmission through the film [38,39]. Within the current study, the observed reduction in WVP can be attributed to the crosslinking and aggregation arising from the additional H-bonds present. The better performances of Cs-ODIN with respect to the Cs-PU counterparts are attributed to the strong self-dimerizing properties of ODIN, which lead to a more effective cross-linking.

### 3.5. Hydrophilic/hydrophobic character

To evaluate the wettability of the films and have more insights into the surface hydrophobicity and interfacial properties of the materials, water contact angle (WCA) measurements were performed. The results of these measurements, as presented in Table 2, indicate that the pristine film exhibits a slight hydrophilic character, with a WCA of 86°. The incorporation of ODIN and PU leads to an increase in hydrophobicity, with a ~ 25° increase in WCA observed for both ODIN-III and PU-III.

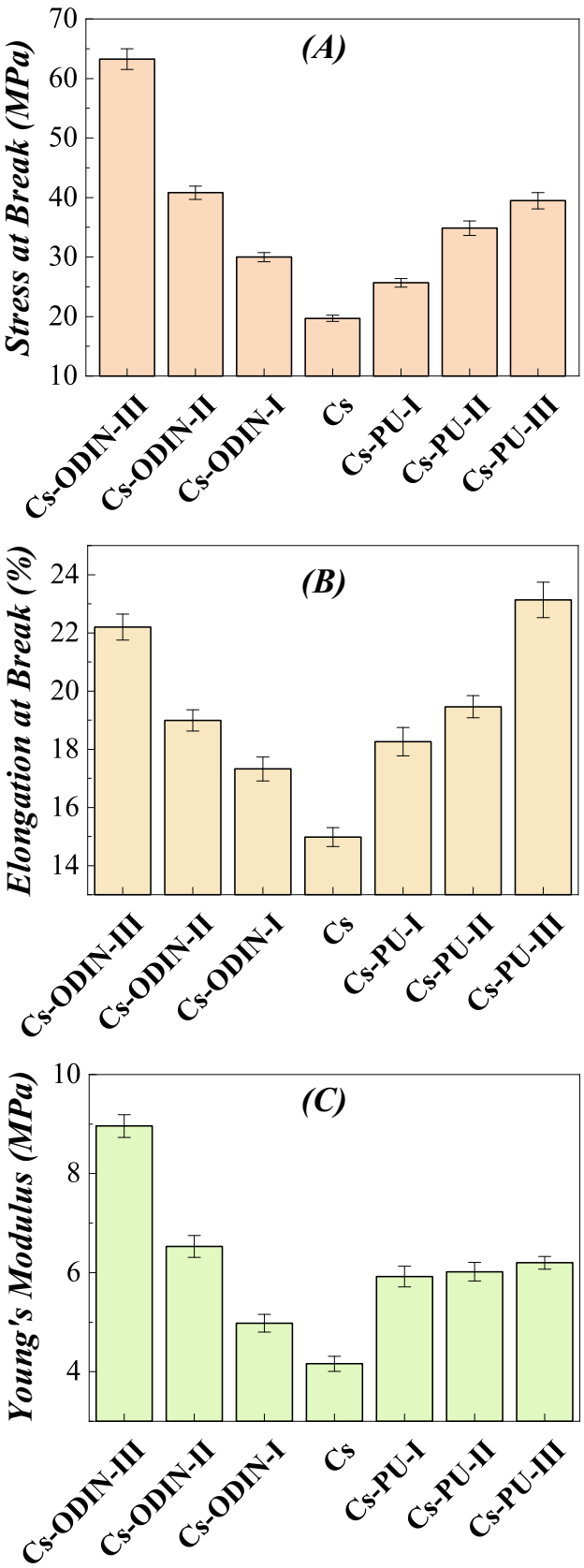


**Fig. 4.** Tensile stress (A), elongation at break (B), and Young's modulus (C) of Cs-modified films. Each value represents the mean ± SD ($n = 3$) of triplicates.

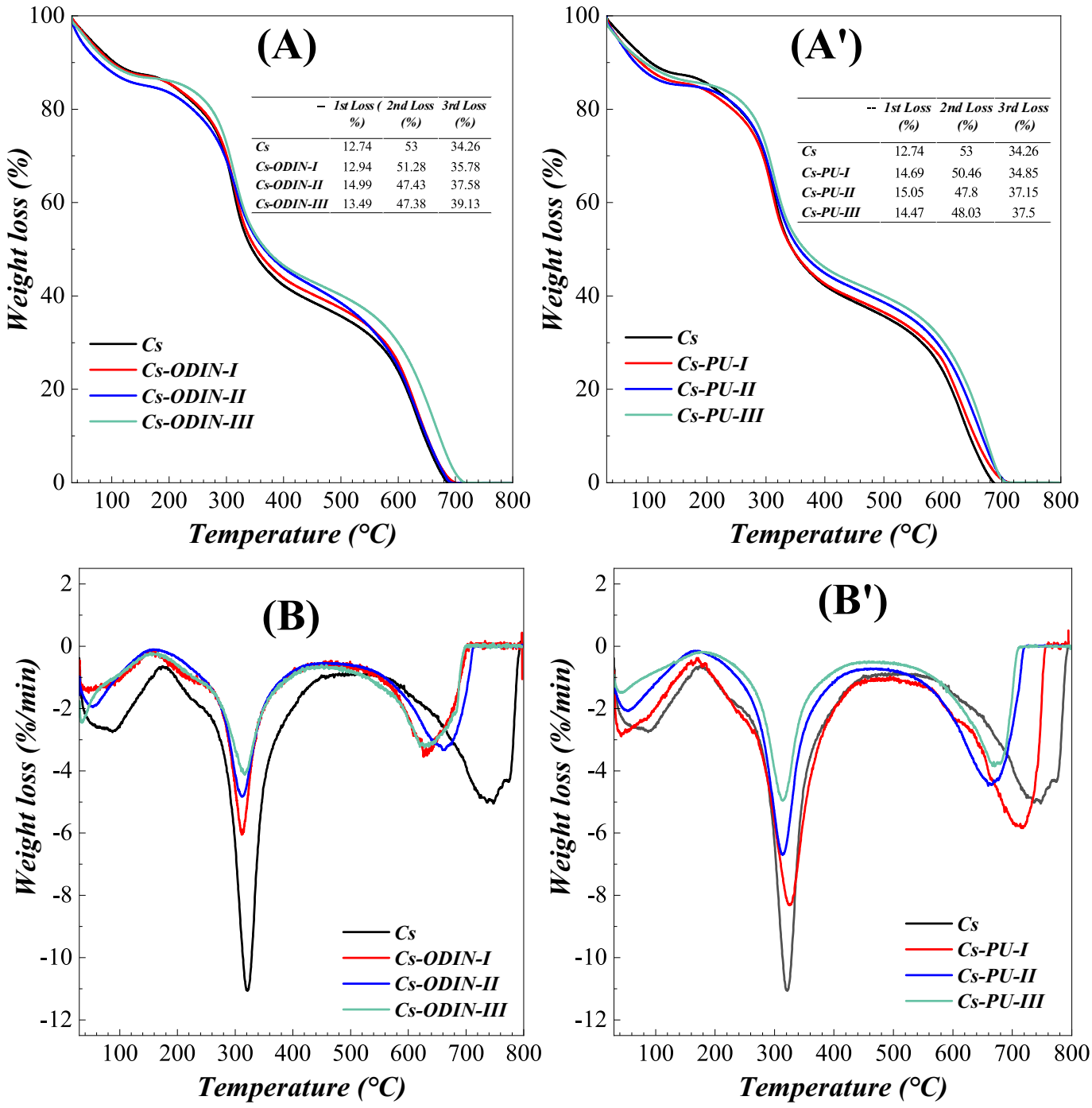


| – | 1st Loss (%) | 2nd Loss (%) | 3rd Loss (%) |
|---|---|---|---|
| Cs | 12.74 | 53 | 34.26 |
| Cs-ODIN-I | 12.94 | 51.28 | 35.78 |
| Cs-ODIN-II | 14.99 | 47.43 | 37.58 |
| Cs-ODIN-III | 13.49 | 47.38 | 39.13 |

| – | 1st Loss (%) | 2nd Loss (%) | 3rd Loss (%) |
|---|---|---|---|
| Cs | 12.74 | 53 | 34.26 |
| Cs-PU-I | 14.69 | 50.46 | 34.85 |
| Cs-PU-II | 15.05 | 47.8 | 37.15 |
| Cs-PU-III | 14.47 | 48.03 | 37.5 |

**Fig. 5.** TGA (upper side) and DTGA (bottom side) curves of modified Cs-ODIN (A and B) and Cs-PU (A′ and B′) films.

Those findings are particularly related to the structure of the incorporated moieties, which bring their hydrophobic character related to the presence of aromatic rings and aliphatic tails in the molecular structure into the final product. A similar hydrophobic increase has been achieved by incorporating hydrophobic compounds, as demonstrated in other chitosan-based materials [13].

### 3.6. Mechanical properties

Tensile stress-strain assessments were carried out on the synthesized films to evaluate the impact of chemical modification on chitosan's mechanical performance. The results are presented in Fig. 4. The mechanical measurements reveal a marked enhancement in tensile strength upon incorporation of ODIN and PU. Specifically, the tensile strength (Fig. 4A) increased by approximately 50 %, 100 %, and 200 % for Cs-ODIN-I, Cs-ODIN-II, and Cs-ODIN-III, respectively. A similar trend was observed for the PU-modified films, with increases of approximately 25 %, 75 %, and 100 % for PU-I, PU-II, and PU-III, respectively. This marked difference in performance can be attributed to the intrinsic molecular characteristics of the two moieties. PU enhances the number of hydrogen bonds within the polymer matrix, contributing to improved interactions between chitosan chains [14,25]. Instead, ODIN exhibits a stronger reinforcing effect due to its ability to self-dimerize, forming supramolecular cross-links. These dimers act as multiple-point cross-linkers, establishing a stronger hydrogen bonding network compared to PU (Chart 1). This higher crosslinking potential likely accounts for the

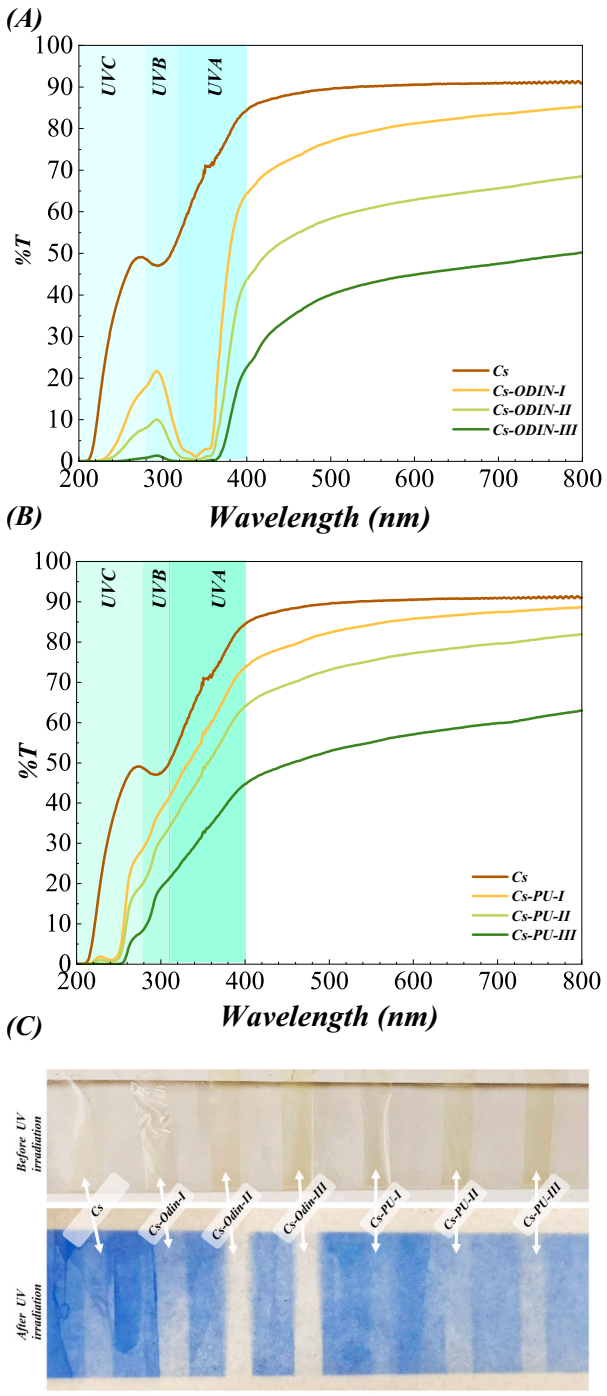


**Fig. 6.** UV–Vis transmission spectrum of Cs-ODIN and Cs-PU films (A and B) and their UV barrier efficiency against UV activated dye (C).

more pronounced improvements in mechanical strength observed in ODIN-based films. Additionally, a comparable increase in elongation at break (Fig. 4B) was observed in both materials, reaching a maximum of approximately 8 % in films with the highest ODIN and PU content. This mechanical behavior is comparable to that of hydrogen-bonded cross-linked chitosan systems incorporating plant extracts or nanoparticles [40,41], suggesting that ODIN and PU act as both crosslinkers and reinforcing agents within the Cs polymer network. Moreover, a significant increase in Young's modulus (Fig. 4C) after modification with ODIN was observed, and, to a minor extent, also with PU. These additives are making the films stiffer, enhancing their ability to withstand mechanical stress without undergoing significant deformation.

**Table 3**
UVA, UVB, and UPF values of Cs Films.

| Samples | UVA (%) | UVB (%) | UPF | Interpretation |
|---|---|---|---|---|
| ***Cs*** | 70.3 ± 3.0 | 48.7 ± 1.7 | 1.95 ± 0.07 | *Very low protection* |
| ***CS-ODIN-I*** | 23.5 ± 1.0 | 15.9 ± 0.5 | 7.68 ± 0.26 | *Low protection* |
| ***CS-ODIN-II*** | 12.9 ± 0.6 | 6.7 ± 0.2 | 19.2 ± 0.6 | *Good protection* |
| ***CS-ODIN-III*** | 5.3 ± 0.2 | 0.72 ± 0.02 | 161.9 ± 1.2 | *Exceptional protection* |
| ***CS-PU-I*** | 59.2 ± 2.5 | 39.0 ± 1.3 | 2.34 ± 0.08 | *Very low protection* |
| ***CS-PU-II*** | 50.5 ± 2.2 | 31.4 ± 1.1 | 2.86 ± 0.10 | *Very low protection* |
| ***CS-PU-III*** | 34.1 ± 1.5 | 19.1 ± 0.6 | 4.53 ± 0.15 | *Very low protection* |

Each value represents the average ± SD from three independent measurements (n = 3).

### 3.7. Thermal stability

The thermal stability of chitosan-based films is a critical parameter that influences processing applications involving elevated temperatures. Assessing thermal stability also provides valuable insights into the structural integrity and thermal degradation behavior of the polymer matrix before and after modification. As shown in Fig. 5A, the TGA curves of all chitosan films display three characteristic stages of weight loss. The first stage, occurring between 100 °C and 120 °C, corresponds to the loss of physically adsorbed water and accounts for approximately 15–18 % of the total mass. The second major weight loss, observed around 350–400 °C, is attributed to the thermal degradation of the chitosan backbone, with an average mass loss of ~40 %. The final stage, at approximately 600 °C, is associated with the decomposition of carbonaceous residues and the oxidative degradation of char in air [42]. A comparative analysis of the TGA profiles reveals a noticeable shift in the degradation temperature during the second stage for the modified films, particularly those containing ODIN and PU. This shift toward higher temperatures indicates enhanced thermal stability following chemical modification, relative to the pristine chitosan [43]. Furthermore, the DTGA curves shown in Fig. 5B corroborate these observations, highlighting similar degradation steps while providing more detail on the rate of degradation. Notably, the Cs–ODIN films exhibit a lower degradation rate compared to the PU-modified films, suggesting superior thermal resistance [44].

### 3.8. UV-Light barrier property

The light barrier properties of the films were determined following the methodology described in the 2.6.1 section in transmission mode. The films exhibit significantly enhanced light barrier properties compared to the pristine chitosan, which typically offers only moderate UV protection. As illustrated in Fig. 6, the Cs-ODIN films show remarkably low UV light transmission throughout the entire UV spectrum, with the Cs-ODIN-III formulation achieving complete (100 %) UV blocking across all UV wavelengths. Instead, the Cs-PU films display comparatively weaker light barrier performances, effectively blocking 100 % of UVC radiation, but providing limited protection against UVA and UVB wavelengths. The UV-blocking capability is demonstrated in Fig. 6C, where Cs-ODIN and Cs-PU films were employed as UV shields to prevent the photoactivation of the nitrospiropyran dye, with Cs-ODIN-III showing outstanding protective performance. To standardize the evaluation of UV protection, the calculation of UVA, UVB transmittance, and UPF values was performed following the AS/NZS 4399 guidelines [29]. Table 3 displays these results, highlighting the superior protective performance of the Cs-ODIN formulations. Cs-ODIN-III achieved an exceptional UPF value of 161.95, indicating excellent UV shielding. This improvement is attributed to its naphthyridine-based structure, which contains a higher number of chromophore groups capable of absorbing UV radiation, compared to the PU counterpart [44]. Furthermore, compared to previously reported chitosan-based films incorporating

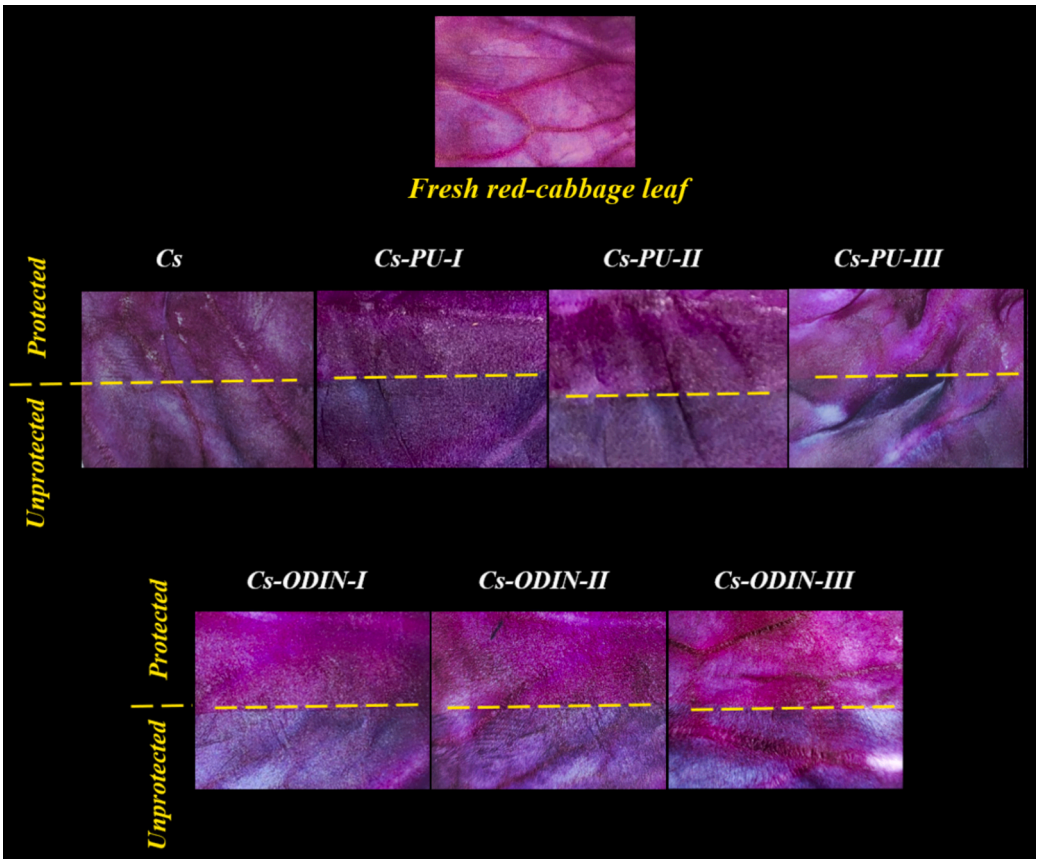


**Fig. 7.** Photographs of red cabbage samples covered with modified Cs films after 6 h of UV irradiation.

lemon essential oil (LEO) and cranberry juice, which demonstrated similar functional enhancements [35], the present study offers a more effective strategy by chemically integrating additives rather than relying on their physical incorporation. Physical blending often leads to the gradual loss of functionality due to additive migration. In contrast, the synthesized additives — particularly ODIN — and their carefully optimized incorporation levels not only achieve comparable or superior performance, but also enhance long-term stability. This makes the approach more practical and durable.

### 3.9. Food protection test (FTP)

For the FPT, we used red cabbage (RCb), which is an anthocyanin-rich vegetable known for its high sensitivity to pH and light, particularly UV radiation, which causes visible color changes. The use of Cs films as barriers to this radiation showed interesting results as reported in Fig. 7. After 6 h of UV radiation, the RCb covered with pristine Cs film exhibited a color change from light purple to a pale dark color due to the degradation of the anthocyanin present in the vegetable. On the other

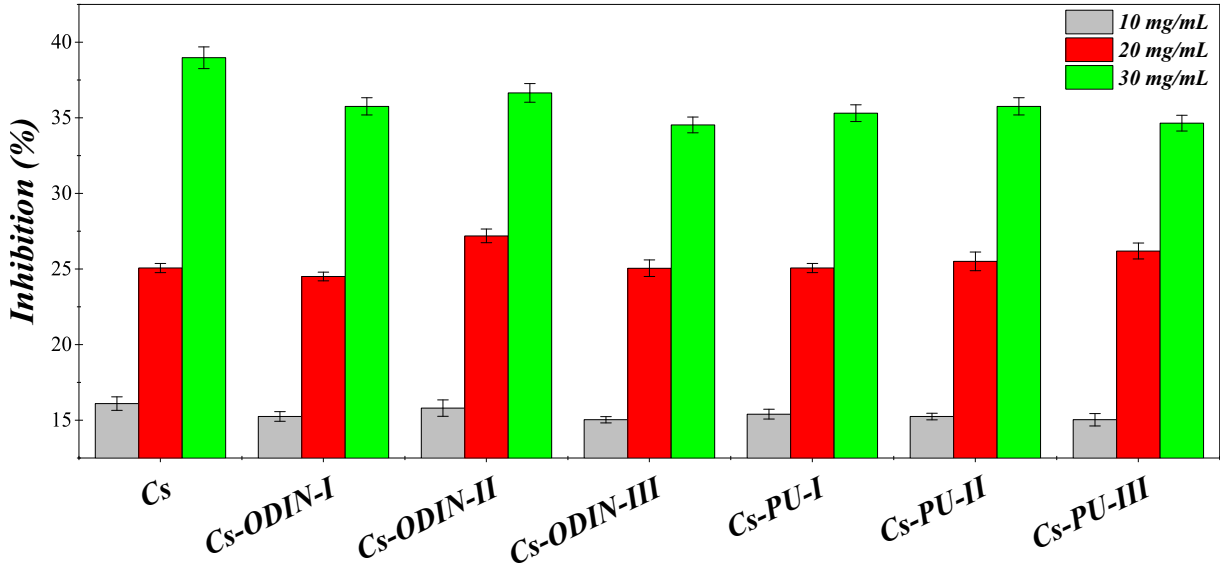


**Fig. 8.** DPPH scavenging activity of modified-Cs films. Each value represents the mean ± SD ($n = 3$).

hand, the modified Cs films presented different protection levels based on the type of modifier and its concentration. In the case of PU, only a limited protective effect is observed even at high PU content, as shown in Fig. 7. In contrast, Cs-ODIN films display markedly reduced discoloration on the covered side compared to the uncovered one, highlighting their effectiveness as a protective barrier against UV-induced degradation. These observations confirm the UPF values previously reported in Table 3, and show that the ODIN-modified chitosan films can contribute to prolonging the freshness and visual appeal of food products.

### 3.10. Antioxidant activity

One of the most widely used methods for evaluating the antioxidant properties of substances is the DPPH radical scavenging assay. The antioxidant acts by neutralizing DPPH free radicals through electron or hydrogen atom donation, resulting in a measurable decrease in absorbance that reflects their scavenging capacity [45]. Fig. 8 illustrates the DPPH radical scavenging activity of the tested films. All the materials exhibited an increasing antioxidant activity as their concentration in the DPPH solution increased. This activity is generally attributed to the free amino (-$NH_2$) and hydroxyl (-OH) groups of chitosan, which react with free radicals to form stable macromolecular radicals [46]. The DPPH radical scavenging activity was not significantly altered by the incorporation of ODIN or PU into the chitosan matrix. However, a slight decrease in activity was observed at certain concentrations, which can be explained by the reduction of free-OH and -$NH_2$ groups after functionalization.

## 4. Conclusion

The incorporation of PU and ODIN into chitosan films significantly improved their functional properties. Both modifiers reduced WVP by 30–40 %, indicating a denser, hydrogen-bonded network. ODIN outperformed PU due to its stronger hydrogen-bonding ability, reflected in higher UVA, UVB, and UPF values, making ODIN-based films especially suited for applications requiring UV protection. This was further confirmed by a preservation test using red cabbage, where ODIN-containing films provided superior protection against UV-induced oxidation compared to both pristine and PU-modified Cs films. Thermal analysis showed improved stability in modified films, with ODIN-based films exhibiting higher degradation temperatures and lower degradation rates than PU films. Mechanical testing revealed substantial increases in tensile strength, elongation at break, and stiffness. For ODIN-modified films, these enhancements were attributed to its dimerization and crosslinking abilities. Overall, ODIN and PU grafting on pristine Cs enhances the films' barrier, optical, thermal, and mechanical performance, making it a promising material for packaging applications. In summary, the introduction of ODIN as a supramolecular dimerizing unit proved to be an effective route to boost chitosan properties.

## CRediT authorship contribution statement

**Mouad El Mouzahim:** Writing – original draft, Methodology, Investigation, Formal analysis, Conceptualization. **Alessandro Pedrini:** Writing – review & editing. **Enrico Dalcanale:** Writing – review & editing, Validation. **A. Jorge Parola:** Writing – review & editing. **Roberta Pinalli:** Writing – review & editing, Validation, Supervision, Funding acquisition.

## Declaration of competing interest

The authors declare that they have no known competing financial interests or personal relationships that could have appeared to influence the work reported in this paper.

## Data availability

Data will be made available on request.

## Acknowledgments

The authors acknowledge the project VIT, funded through the European Union Horizon 2020 Program (H2020-MSCA-RISE-2020, grant agreement no. 101008237). This work also benefited from the equipment and support provided by the COMP-HUB and COMP-R Initiatives, funded under the 'Departments of Excellence' program of the Italian Ministry of University and Research (MIUR, 2018–2022; MUR, 2023–2027). The authors further acknowledge the Centro Interfacoltà di Misure "G. Casnati" of the University of Parma for access to NMR facilities. The first author acknowledges National Recovery and Resilience Plan (NRRP), Mission 4 Component 2 Investment 3.3 - Call for tender No. 352 of 09/04/2022 of Italian Ministry of University and Research funded by the European Union – NextGenerationEU and INTERCOS group for the financial support. Special thanks are extended to **Dr. Ilaria Ferraboschi** from the Department of Chemistry, Life Sciences, and Environmental Sustainability of the University of Parma, for her valuable support with two-photon microscopy imaging, which contributed significantly to this work. The authors also thank **Professor Dr. Luísa Neves** of the NOVA School of Science and Technology, Lisbon, for kindly providing access to the scanning electron microscopy (SEM) facility, and **Professor Dr. Filomena Freitas**, of the same institution, for granting access to the texturometer, both of which were essential to the successful completion of this study.

## Appendix A. Supplementary data

Supplementary data to this article can be found online at https://doi.org/10.1016/j.ijbiomac.2025.149060.

## References

[1] Q. Chen, Y. Qi, Y. Jiang, W. Quan, H. Luo, K. Wu, S. Li, Q. Ouyang, Progress in research of chitosan chemical modification technologies and their applications, Mar. Drugs 20 (8) (2022) 536, https://doi.org/10.3390/md20080536.
[2] R. de Sousa Victor, Marcelo da Cunha, A. Santos, B. Viana de Sousa, G. de Araújo Neves, Navarro de Lima, L. Santana, R. Rodrigues Menezes, A review on chitosan's uses as biomaterial: tissue engineering, drug delivery systems and cancer treatment, Materials 13 (21) (2020) 4995, https://doi.org/10.3390/ma13214995.
[3] P. Baharlouei, A. Rahman, Chitin and chitosan: prospective biomedical applications in drug delivery, cancer treatment, and wound healing, Mar. Drugs 20 (7) (2022) 460, https://doi.org/10.3390/md20070460.
[4] J. Su, W. Zhang, Z. Moradi, M. Rouhi, E. Parandi, F. Garavand, Recent functionality developments of carboxymethyl chitosan as an active food packaging film material, Food Chem. (2024) 141356, https://doi.org/10.1016/j.foodchem.2024.141356.
[5] F. Tamzid, S.B. Sakhawat, T.U. Rashid, Chitosan based electrospun nanofibrous materials: a sustainable alternative for food packaging, Trends Food Sci. Technol. (2024) 104617, https://doi.org/10.1016/j.tifs.2024.104617.
[6] W. Zhang, A. Khan, P. Ezati, R. Priyadarshi, M.A. Sani, N.B. Rathod, G. Goksen, J.-W. Rhim, Advances in sustainable food packaging applications of chitosan/polyvinyl alcohol blend films, Food Chem. 443 (2024) 138506, https://doi.org/10.1016/j.foodchem.2024.138506.
[7] I. Aranaz, A.R. Alcántara, M.C. Civera, C. Arias, B. Elorza, A. Heras Caballero, N. Acosta, Chitosan: an overview of its properties and applications, Polymers 13 (19) (2021) 3256, https://doi.org/10.3390/polym13193256.
[8] S. Fathi-Karkan, S. Mirinejad, F. Ulucan-Karnak, M. Mukhtar, H.G. Almanghadim, S. Sargazi, A. Rahdar, A.M. Díez-Pascual, Biomedical applications of aptamer-modified chitosan nanomaterials: an updated review, Int. J. Biol. Macromol. 238 (2023) 124103, https://doi.org/10.1016/j.ijbiomac.2023.124103.
[9] S. Dimassi, N. Tabary, F. Chai, N. Blanchemain, B. Martel, Sulfonated and sulfated chitosan derivatives for biomedical applications: a review, Carbohydr. Polym. 202 (2018) 382–396, https://doi.org/10.1016/j.carbpol.2018.09.011.
[10] C. Van Poucke, E. Verdegem, S. Mangelinckx, C.V. Stevens, Synthesis and unambiguous NMR characterization of linear and branched N-alkyl chitosan derivatives, Carbohydr. Polym. 337 (2024) 122131, https://doi.org/10.1016/j.carbpol.2024.122131.
[11] Y. Wang, X. Zhou, J. Jiang, T. Zhao, J. Dang, R. Hu, C. Shen, Q. Fan, D. Sun, M. Zhang, Carboxymethyl chitosan-enhanced multi-level microstructured composite hydrogel scaffolds for bone defect repair, Carbohydr. Polym. 348 (2025) 122847, https://doi.org/10.1016/j.carbpol.2024.122847.

[12] G. Zhao, T. Gu, L. Chen, L. Wang, Y.V. Petrov, V.E. Baulin, A.Y. Tsivadze, D. Jia, Y. Zhou, B. Li, Synergistic adhesion enhancement of double-crosslinking chitosan hydrogel via catechol-Fe3+ coordination and Schiff base, Carbohydr. Polym. 356 (2025) 123380, https://doi.org/10.1016/j.carbpol.2025.123380.
[13] T. Liu, J. Xue, R. Qin, L. Jiang, Bioinspired hydrophobic chitosan-based films for monitoring the visual freshness of pork, Food Hydrocoll. 162 (December 2024) (2025) 110932, https://doi.org/10.1016/j.foodhyd.2024.110932.
[14] Y. Qin, Y. Wang, Z. Tang, K. Chen, Z. Wang, G. Cheng, H. Chi, T. Soteyome, A pH-sensitive film based on chitosan/gelatin and anthocyanin from Zingiber striolatum Diels for monitoring fish freshness, Food Chem. X 23 (July) (2024) 101639, https://doi.org/10.1016/j.fochx.2024.101639.
[15] D. Yu, I.B. Basumatary, S. Kumar, F. Ye, J. Dutta, Chitosan modified with bio-extract as an antibacterial coating with UV filtering feature, Int. J. Biol. Macromol. 230 (January) (2023) 123145, https://doi.org/10.1016/j.ijbiomac.2023.123145.
[16] M. Barik, G.V.S. BhagyaRaj, K.K. Dash, R. Shams, A thorough evaluation of chitosan-based packaging film and coating for food product shelf-life extension, J. Agric. Food Res. 16 (2024) 101164, https://doi.org/10.1016/j.jafr.2024.101164.
[17] Z. Liu, S. Wang, H. Liang, J. Zhou, M. Zong, Y. Cao, W. Lou, A review of advancements in chitosan-essential oil composite films: better and sustainable food preservation with biodegradable packaging, Int. J. Biol. Macromol. (2024) 133242, https://doi.org/10.1016/j.ijbiomac.2024.133242.
[18] U.M. Thiyagamoorthy, G. Sadayandi, S. Jeyaraj, S. Thangarasu, M.A. Wadaan, A. Baabbad, K.M. Vafaeva, J.S. Packialakshmi, Exploring the efficacy of various essential oils in chitosan-based composite biopolymer films for food packaging, Polym. Adv. Technol. 35 (4) (2024) e6371, https://doi.org/10.1002/pat.6371.
[19] C. Rodrigues, J. Maria, M. De Mello, F. Dalcanton, D. Lusitâneo, P. Macuvele, N. Padoin, M. Antônio, C. Soares, Mechanical, thermal and antimicrobial properties of chitosan-based-nanocomposite with potential applications for food packaging, J. Polym. Environ. (2020) 0123456789, https://doi.org/10.1007/s10924-020-01678-y.
[20] X. Sun, H. Wang, H. Liang, N. Meng, N. Zhou, Fabrication of antimicrobial chitosan/ZnO nanoparticles/lecithin-montmorillonite films for food packaging application, Food Hydrocoll. 159 (2025) 110686, https://doi.org/10.1016/j.foodhyd.2024.110686.
[21] J.F. Rubilar, R.M.S. Cruz, R.N. Zuñiga, I. Khmelinskii, M.C. Vieira, Mathematical modeling of gallic acid release from chitosan films with grape seed extract and carvacrol, Int. J. Biol. Macromol. 104 (2017) 197–203, https://doi.org/10.1016/j.ijbiomac.2017.05.187.
[22] J. Tellers, S. Canossa, R. Pinalli, M. Soliman, J. Vachon, E. Dalcanale, Dynamic cross-linking of polyethylene via sextuple hydrogen bonding array, Macromolecules 51 (19) (2018) 7680–7691, https://doi.org/10.1021/acs.macromol.8b01715.
[23] S. D'Auria, A. Pedrini, I. Ferraboschi, J. Vachon, C. Sissa, R. Pinalli, E. Dalcanale, Two-photon microscopy as a visual tool for polymer compatibilization monitoring: the PE-EVOH case, Soft Matter 19 (10) (2023) 1900–1906, https://doi.org/10.1039/d2sm01577c.
[24] A. Okuniewski, J. Chojnacki, B. Becker, N-Benzoyl-N′-phenyl-urea, Acta Crystallogr. E 66 (2) (2010) o414, https://doi.org/10.1107/S1600536810001807.
[25] Y. Wu, Y. Shi, H. Wang, Urea as a hydrogen bond producer for fabricating mechanically very strong hydrogels, Macromolecules 56 (12) (2023) 4491–4502, https://doi.org/10.1021/acs.macromol.3c00611.
[26] M. Lahimer, N. Ayed, J. Horriche, S. Belgaied, Characterization of plastic packaging additives: food contact, stability and toxicity, Arab. J. Chem. 50 (2013), https://doi.org/10.1016/j.arabjc.2013.07.022.
[27] J. Liu, S. Liu, Q. Wu, Y. Gu, J. Kan, C. Jin, Effect of protocatechuic acid incorporation on the physical, mechanical, structural and antioxidant properties of chitosan film, Food Hydrocoll. 73 (2017) 90–100, https://doi.org/10.1016/j.foodhyd.2017.06.035.
[28] X. Zhang, Y. Liu, H. Yong, Y. Qin, J.J. Liu, J.J. Liu, Development of multifunctional food packaging films based on chitosan, TiO2 nanoparticles and anthocyanin-rich black plum peel extract, Food Hydrocoll. 94 (2019) 80–92, https://doi.org/10.1016/j.foodhyd.2019.03.009.
[29] P. Gies, T. Slevin, S. Harrison, P. Plowman, S. Dain, L. Moller, F. Mawley, N. Swift, Australian/New Zealand Standard, AS/NZS 4399: 2017: Sun Protective Clothing–Evaluation and Classification, Standards Australia, 2017.
[30] S. Van Nguyen, B.-K. Lee, PVA/CNC/TiO2 nanocomposite for food-packaging: improved mechanical, UV/water vapor barrier, and antimicrobial properties, Carbohydr. Polym. 298 (2022) 120064, https://doi.org/10.1016/j.carbpol.2022.120064.
[31] X. Wang, H. Yong, L. Gao, L. Li, M. Jin, J. Liu, Preparation and characterization of antioxidant and pH-sensitive films based on chitosan and black soybean seed coat extract, Food Hydrocoll. 89 (August 2018) (2019) 56–66, https://doi.org/10.1016/j.foodhyd.2018.10.019.
[32] Z. Kalaycıoğlu, E. Torlak, G. Akın-Evingür, İ. Özen, F.B. Erim, Antimicrobial and physical properties of chitosan films incorporated with turmeric extract, Int. J. Biol. Macromol. 101 (2017) 882–888, https://doi.org/10.1016/j.ijbiomac.2017.03.174.
[33] B.U. Chaudhary, S. Lingayat, A.N. Banerjee, R.D. Kale, Development of multifunctional food packaging films based on waste garlic peel extract and chitosan, Int. J. Biol. Macromol. 192 (October) (2021) 479–490, https://doi.org/10.1016/j.ijbiomac.2021.10.031.
[34] S. Roy, J.W. Rhim, Preparation of carbohydrate-based functional composite films incorporated with curcumin, Food Hydrocoll. 98 (July 2019) (2020) 105302, https://doi.org/10.1016/j.foodhyd.2019.105302.
[35] K. Odjo, Q.A. Al-Maqtari, H. Yu, Y. Xie, Y. Guo, M. Li, Y. Du, K. Liu, Y. Chen, W. Yao, Preparation and characterization of chitosan-based antimicrobial films containing encapsulated lemon essential oil by ionic gelation and cranberry juice, Food Chem. 397 (2022) 133781, https://doi.org/10.1016/j.foodchem.2022.133781.
[36] M.P. Arrieta, J. López, S. Ferrándiz, M.A. Peltzer, Characterization of PLA-limonene blends for food packaging applications, Polym. Test. 32 (4) (2013) 760–768, https://doi.org/10.1016/j.polymertesting.2013.03.016.
[37] X. Dai, S. Li, S. Li, K. Ke, J. Pang, C. Wu, Z. Yan, High antibacterial activity of chitosan films with covalent organic frameworks immobilized silver nanoparticles, Int. J. Biol. Macromol. 202 (2022) 407–417, https://doi.org/10.1016/j.ijbiomac.2021.12.174.
[38] M. Kurek, I.E. Garofulić, M.T. Bakić, M. Ščetar, V.D. Uzelac, K. Galić, Development and evaluation of a novel antioxidant and pH indicator film based on chitosan and food waste sources of antioxidants, Food Hydrocoll. 84 (2018) 238–246, https://doi.org/10.1016/j.foodhyd.2018.05.050.
[39] S. Sahraee, J.M. Milani, B. Ghanbarzadeh, H. Hamishehkar, Physicochemical and antifungal properties of bio-nanocomposite film based on gelatin-chitin nanoparticles, Int. J. Biol. Macromol. 97 (December) (2017) 373–381, https://doi.org/10.1016/j.ijbiomac.2016.12.066.
[40] Y. Amaregouda, K. Kamanna, T. Gasti, Fabrication of intelligent/active films based on chitosan/polyvinyl alcohol matrices containing Jacaranda cuspidifolia anthocyanin for real-time monitoring of fish freshness, Int. J. Biol. Macromol. 218 (2022) 799–815, https://doi.org/10.1016/j.ijbiomac.2022.07.174.
[41] N.G. Madian, N. Mohamed, Enhancement of the dynamic mechanical properties of chitosan thin films by crosslinking with greenly synthesized silver nanoparticles, J. Mater. Res. Technol. 9 (6) (2020) 12970–12975, https://doi.org/10.1016/J.JMRT.2020.09.028.
[42] F. Bi, X. Zhang, R. Bai, Y. Liu, J. Liu, J. Liu, Preparation and characterization of antioxidant and antimicrobial packaging films based on chitosan and proanthocyanidins, Int. J. Biol. Macromol. 134 (2019) 11–19, https://doi.org/10.1016/j.ijbiomac.2019.05.042.
[43] J.A. Sirviö, A.M. Kantola, S. Komulainen, S. Filonenko, Aqueous modification of chitosan with itaconic acid to produce strong oxygen barrier film, Biomacromolecules 22 (5) (2021) 2119–2128, https://doi.org/10.1021/acs.biomac.1c00216.
[44] L. Xiao, X. Xing, Z. Chen, B. Qu, H. Lan, Q. Gong, J. Kido, Highly efficient electron-transporting/injecting and thermally stable naphthyridines for organic electrophosphorescent devices, Adv. Funct. Mater. 23 (10) (2013) 1323–1330, https://doi.org/10.1002/adfm.201202194.
[45] K. Saravanakumar, A. Sathiyaseelan, A.V.A. Mariadoss, H. Xiaowen, M.-H. H. Wang, Physical and bioactivities of biopolymeric films incorporated with cellulose, sodium alginate and copper oxide nanoparticles for food packaging application, Int. J. Biol. Macromol. 153 (2020) 207–214, https://doi.org/10.1016/j.ijbiomac.2020.02.250.
[46] J.T. Martins, M.A. Cerqueira, A.A. Vicente, Influence of α-tocopherol on physicochemical properties of chitosan-based films, Food Hydrocoll. 27 (1) (2012) 220–227, https://doi.org/10.1016/j.foodhyd.2011.06.011.